Heliyon 9 (2023) e13182

Contents lists available at ScienceDirect

Heliyon

journal homepage: www.cell.com/heliyon

Research article

A LSTM-RNN based intelligent control approach for temperature and humidity environment of urban utility tunnels

Fang-Le Peng [a], Yong-Kang Qiao [a,*], Chao Yang [a,b]

[a] Research Center for Underground Space & Department of Geotechnical Engineering, Tongji University, Shanghai 200092, PR China
[b] Roads & Bridges Branch, China MCC5 Group Corp. Ltd., Chengdu 610066, PR China

ARTICLE INFO

Keywords:
Urban utility tunnel
Temperature
Relative humidity
Ventilation
LSTM

ABSTRACT

Temperature and relative humidity are important indicators of utility tunnel indoor atmosphere hazards and operational risks, which can be effectively mitigated by accurate forecasting and corrective control measures. To this end, this paper proposed a multi-layer long short-term memory (LSTM) recurrent neural network (RNN) architecture to forecast the changing trend of temperature and relative humidity inside utility tunnels with distant past monitoring data. Based on the forecasting architecture, an intelligent control approach was designed, including early warning and ventilation control measures. Case study results showed that the proposed architecture fit the training dataset well and the prediction accuracy on testing datasets of temperature and relative humidity exceeded 98% and 99%, respectively. Meanwhile, the proposed LSTM-RNN architecture can also be used to simulate and evaluate the ventilation effects on the temperature and relative humidity environment of urban utility tunnels. Findings of this paper provide a reference for the safe, efficient and energy-saving indoor environment control of urban utility tunnels.

1. Introduction

As a key urban infrastructure housing various municipal pipelines, urban utility tunnels are widely considered a sustainable and resilient solution to traditional overhead or trenching practices [1–5]. Inside such a long, narrow and enclosed underground space, air quality tends to be worsened by harmful substances accumulating with poor air circulation, which poses a threat to the facilities, equipment and people entering utility tunnels [6]. Current literature shows that temperature and relative humidity are important indicators of utility tunnel indoor atmosphere hazards and operational risks [7]. For instance, a high humidity environment can increase the growth rate of harmful microorganisms [8,9], and the probability of pipeline corrosion and electronic component damage [10]. Also, a high temperature environment is likely to result in short circuits and fires of electricity/telecom cables [11,12].

Ventilation is an effective means to improve air quality and to mitigate indoor atmosphere hazards and operational risks [13]. To optimize the ventilation design of utility tunnels, CFD simulation models [14] and scaled models [15,16] were used to simulate the temperature and humidity environment. But such simulation methods cannot be used in real-time forecasting. Toward the effective governance of utility tunnels, a comprehensive monitoring system framework was proposed for the real-time analysis of temperature and humidity indicators [17], based on which tunnel managers could take preventive and corrective ventilation control measures. However, the best time and duration of ventilation control cannot be accurately estimated simply depending on human experience,

* Corresponding author.
E-mail addresses: qiaoyongkang@tongji.edu.cn, iamqyk@163.com (Y.-K. Qiao).

https://doi.org/10.1016/j.heliyon.2023.e13182
Received 23 September 2022; Received in revised form 19 January 2023; Accepted 19 January 2023
Available online 25 January 2023

which may lead to poor ventilation effects and energy waste. Given the characteristics of time-varying, hysteresis and nonlinearity of ventilation system [18], the ventilation control approach of utility tunnels should build on the accurate forecasting of the changing trend of temperature and humidity environment. Such an approach is determined by many factors, such as internal temperature and humidity conditions, external temperature and humidity conditions, and ventilation states. To date, however, little attention has been paid to the accurate forecasting and the dynamic ventilation control approach for the temperature and humidity environment of urban utility tunnels.

Recurrent neural network (RNN) is a classical deep learning model. It processes sequence input data cyclically through a basic neural network cell [19]. Long short-term memory (LSTM) model is a special variation of RNN, proposed to solve the problems of gradient vanishing and exploding in traditional RNN structure during the long-sequence training process [20,21]. Therefore, LSTM-RNN is able to mine rules from distant past sequence data. Through model training, it can accurately forecast the changing trend of data [22]. Since the analyzed data in this study is sequential with long-range dependencies, a LSTM-RNN based architecture is suited for the temperature and relative humidity forecasting problem of utility tunnels.

Against the aforementioned background, this paper proposes a novel approach for the intelligent ventilation control of the temperature and humidity environment inside urban utility tunnels using a LSTM-RNN based real-time and dynamic forecasting architecture. This paper is structured as follows. Section 2 lists the requirements for the intelligent control of temperature and humidity environment in utility tunnels. Section 3 explains in detail the methodology of the proposed approach, which is then illustrated by an empirical case study in a city located in Guizhou Province, China in Section 4. It is hoped that the proposed approach will provide a good reference for addressing the issues of utility tunnel indoor atmosphere hazards and operational risks, facilitating the healthy and energy-saving indoor environment control, and achieving the safe and sustainable operation of urban utility tunnels.

2. Requirements of temperature and humidity environment control in utility tunnels

2.1. Influencing factors of temperature and humidity environment in utility tunnels

Air temperature inside utility tunnels is mainly influenced by the heat sources inside and outside the tunnel, such as external air, surrounding soil, tunnel structure, high-energy pipelines (e.g., high-voltage electricity cables and heating pipelines as often accommodated in a typical utility tunnel shown in Fig. 1), etc. Relative humidity rise inside utility tunnels is often caused by the water vapor from external air or internal water evaporation. The principal influencing factors of the temperature and humidity environment in utility tunnels are summarized and analyzed in Table 1.

It can be seen from Table 1 that the influencing factors of temperature and humidity environment in utility tunnels can be broadly grouped into two types based on the manageability. For such factors as utility services (including cables and pipelines), related equipment and surrounding soil, they are hard, if not impossible, to manage or control once utility tunnels are implemented. In comparison, the control of temperature and humidity environment are more likely to be achieved by optimizing the exchange of internal and external air, i.e., ventilation, contingent upon the external and internal temperature and humidity environment.

2.2. Ventilation system of utility tunnels

In general, a utility tunnel is separated into several fire compartments [23], and both ends of a fire compartment are blocked by fire partition walls and fire doors to form a relatively separate enclosed space. The common forms of utility tunnel ventilation system involve natural air intake and mechanical exhaust [7] as shown in Fig. 2. External air enters from a natural air inlet shaft at one end of a fire compartment into the tunnel space, flows under the thermal pressure and wind pressure, and is exhausted by mechanical exhaust fans from an air outlet shaft at the other end.

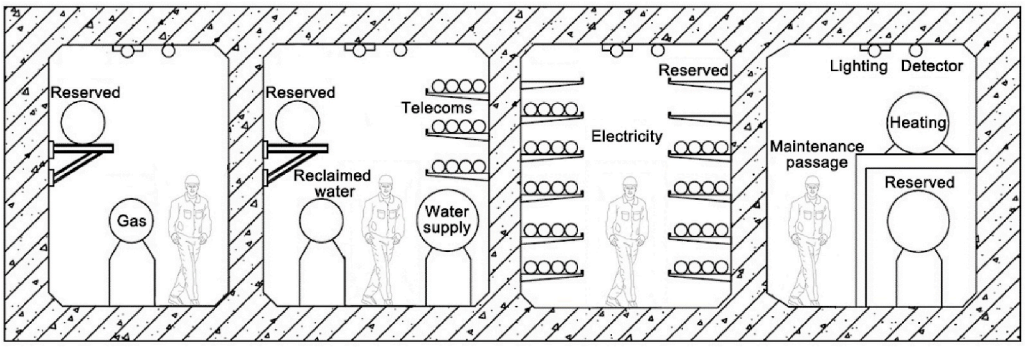

Fig. 1. A typical cross section of a utility tunnel.

Table 1
Influencing factors of temperature and humidity environment in utility tunnels.

	Influencing factors	Influencing mechanisms
Temperature	External air temperature	Heat convection due to temperature difference between internal and external air
	High-voltage cables	Heat radiation from electricity cables
	Heating pipelines	Heat radiation from heating pipelines
	Surrounding soil	Heat conduction due to temperature difference between tunnel structure and surrounding soil
	Ventilation	Accelerated heat convection rate due to ventilation
	Equipment	Heat radiation from equipment operation
Relative humidity	Internal air temperature	Accelerated internal water evaporation rate due to high temperature
	External air humidity	Water vapor exchange due to relative humidity difference between internal and external air
	Air pressure	Increased relative humidity due to decreased air pressure
	Water leakage	Increased water evaporation from water leakage
	Ventilation	Accelerated rates of water vapor exchange and water evaporation

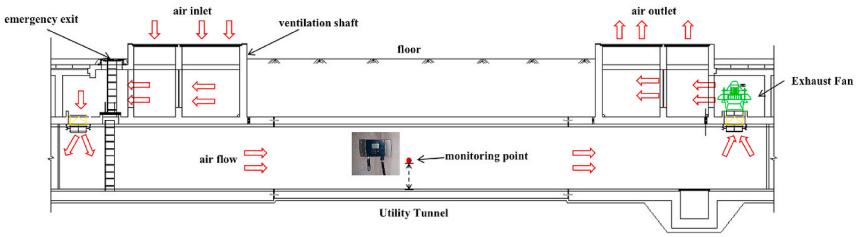

Fig. 2. Schematic diagram of utility tunnel ventilation system.

2.3. Control strategies for utility tunnel ventilation

The starting time and duration of ventilation operation have great influence on the temperature and humidity environment inside utility tunnels. Improper ventilation strategies may even worsen the environment or cause energy waste. This is particularly true during winter and summer when temperature difference inside and outside utility tunnels is generally large. In winter, external cold air introduced into tunnels by ventilation system can lead to a rapid drop in temperature, which increases the risk of frost crack of pipelines due to thermal expansion and cold contraction. In summer, ventilation system intakes saturated hot air into tunnels, causing severe condensation of vapor on the surface of pipelines, equipment and concrete structure (see Fig. 3), which will accelerate corrosion and microbe growth inside utility tunnels.

Base on the aforementioned analysis, some basic control strategies for utility tunnel ventilation system can be obtained as follows. These strategies should also be integrated into the forecasting architecture and the ventilation control approach to be proposed in this study.

(1) Internal and external temperature and humidity conditions should be considered.

Fig. 3. Condensation phenomenon inside utility tunnels in summer.

(2) The effectiveness of ventilation should be pre-estimated before starting the fans.
(3) The starting time and duration of ventilation operation should be forecasted accurately.

2.4. Early warning thresholds of temperature and humidity environment in utility tunnels

Toward the effective ventilation control in utility tunnels, early warning thresholds of temperature and humidity environment should be determined beforehand. In this study, the early warning thresholds are categorized into conventional thresholds and comfort thresholds. The conventional thresholds satisfy the requirements of utility safe operation during the period without person entry, while the comfort thresholds address the needs of human comfort when there are people in tunnels. According to Chinese standards and specifications, the temperature range of a conventional threshold is 5–40 °C, and the relative humidity should not exceed 65% [24]. The temperature range of a comfort threshold is 15–30 °C, and relative humidity should be within the range of 30–60% [25].

According to the highest value in the prediction sequence in the follow-up case scenario and the aforementioned thresholds, this paper identifies three warning levels and the corresponding control measures as listed in Table 2. Under the first level warning, we should pay more attention to the monitoring data, but do not necessarily need to take measures. Under the second level warning, ventilation feasibility should be assessed to send the right signals to start the fans. Under the third level warning, the de-humidification measures must be taken immediately, and patrol personnel should be sent to the corresponding sections to find out the causes and check potential safety hazards such as short circuit and corrosion.

3. Methodology

3.1. Long short-term memory

The LSTM cell is mainly composed of input gate, forget gate and output gate (see Fig. 4). These gates have the following functions:

(1) The input gate i decides how much new information from the current input x_t is to be added to the current cellular state c_t based on the previous hidden state $h_{t\text{-}1}$ by Eqs. (1) and (2):

$$i_t = sigmoid(W_i \cdot x_t + U_i \cdot h_{t-1} + b_i) = \sigma(\widehat{i}_t) \tag{1}$$

$$a_t = tanh(W_c \cdot x_t + U_i \cdot h_{t-1} + b_c) = tanh(\widehat{a}_t) \tag{2}$$

(2) The forget gate f decides what information of the previous cellular state $c_{t\text{-}1}$ is to be deleted, and how the previous cellular state $c_{t\text{-}1}$ is updated to the current cellular state c_t by Eqs. (3) and (4):

$$f_t = sigmoid\left(W_f \cdot x_t + U_f \cdot h_{t-1} + b_f\right) = \sigma(\widehat{f}_t) \tag{3}$$

$$c_t = f_t \odot c_{t-1} + i_t \odot a_t \tag{4}$$

(3) The output gate o decides how the current cellular state c_t influences the current output hidden state h_t by Eqs. (5) and (6):

$$o_t = sigmoid(W_o \cdot x_t + U_o \cdot h_{t-1} + b_o) = \sigma(\widehat{o}_t) \tag{5}$$

$$h_t = o_t \cdot tanh(c_t) \tag{6}$$

where W^*, U^*, b^* are the weight matrixes of gates, the weight matrixes of hidden states, and the biases of gates; a_t describes the cellular state under the current input; t represents the current time step; $\odot$ is an element-wise multiplier and σ represents the sigmoid activation function.

Table 2
Warning level classification.

Conventional threshold	Temperature [°C]	>35	>40	<5 or >45
	Relative humidity [%]	>65	>75	>90
Comfort threshold	Temperature [°C]	<15 or >30	<10 or >35	<5 or >40
	Relative humidity [%]	>60 or <30	>70	>80
Warning level		I	II	III

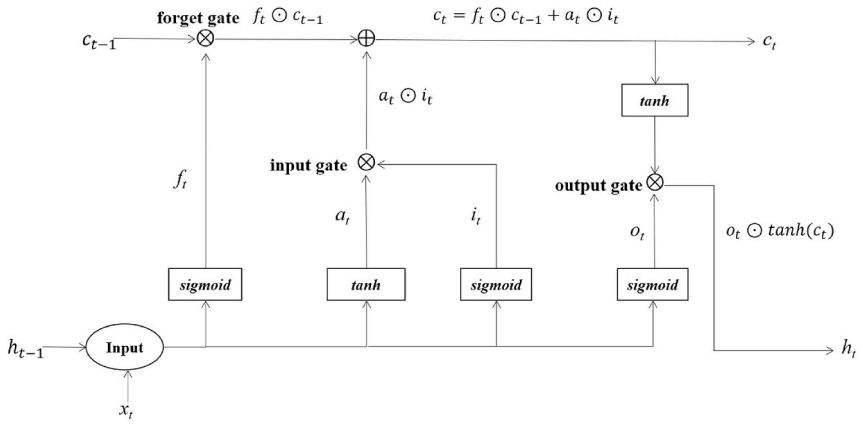

Fig. 4. Basic structure of a LSTM cell.

3.2. LSTM-RNN based forecasting architecture

The LSTM-RNN based forecasting architecture proposed for temperature and humidity indicators of utility tunnels includes five parts as shown in Fig. 5: input layer, hidden layer, output layer, model training and model prediction.

(1) The input layer involves data preprocessing and feature engineering. As has been analyzed in Section 2, the raw data input to forecast the temperature and humidity inside utility tunnels include the data collecting time and location (e.g., tunnels section and fire compartment), external temperature, internal temperature, external relative humidity, internal humidity and the status of ventilation fans. Data preprocessing solves the problems such as the disunity of data units, data missing and noise. Feature engineering transforms the original raw data into the training dataset and testing dataset for the LSTM-RNN forecasting

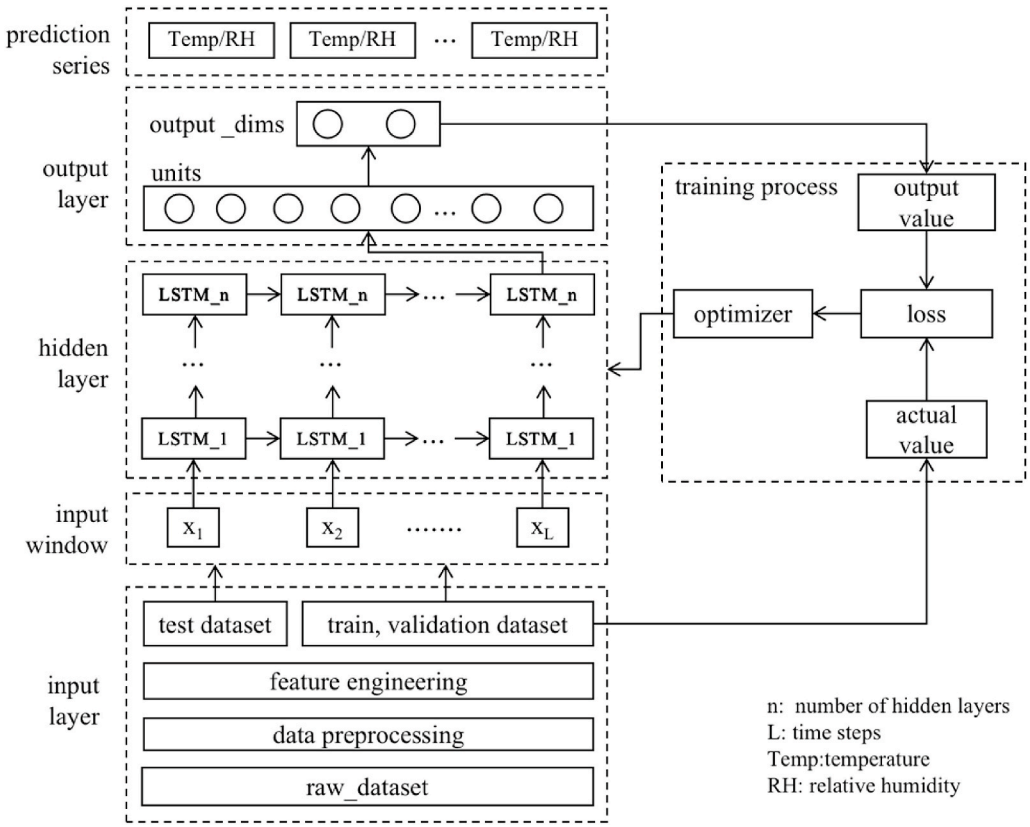

Fig. 5. LSTM-RNN based forecasting architecture.

architecture. Considering unit inconsistency, the input feature data should be normalized before the model training process. The following Eq. (7) is used to scale the data values into [0, 1].

$$x_t^{'} = \frac{x_t - x_{\min}}{x_{\max} - x_{\min}} \tag{7}$$

where $x_t^{'}$ represents the normalized data value at time step t, x_t is the original data value before normalization, $x_{\min}$ and $x_{\max}$ are the minimum and maximum values of the dataset to be normalized.

(2) The hidden layer is the core of the architecture. In the proposed architecture, the hidden layer is a recurrent neural network composed of multi-layer LSTM, and its super parameters include the number of hidden layers n, the number of hidden variable units and time steps L. The parameters of hidden layers n and the number of units reflect the complexity of the model and need to be determined according to the model tuning results, while time steps L is related to the analysis requirements and the characteristics of data [26].

(3) The output layer is used to decode the analysis results of the hidden layer and output the decoding results in fixed dimensions. It can be fully a connected layer or convolution layer, and the output dimension is determined by the variable dimension to be predicted. For this study, the output dimension is two as only temperature and relative humidity are the expected forecasting indicators.

(4) Model training is processed based on the difference between the output results and the actual data (i.e. loss function) of the output layer. Back-propagation through time (BPTT) algorithm is used to calculate the partial derivatives of the loss function to the model parameters of LSTM cells. According to the partial derivatives, model parameters are updated in each BPTT process iteratively by gradient optimizers until convergence. The gradient optimizer adopted in the proposed architecture is the Adam optimizer, which can compute adaptive learning rates for different parameters and work well with sparse gradients [27].

(5) Model prediction process applies the trained model to predict and analyze the changing trend of temperature and humidity inside utility tunnels in real-time. The prediction output is a forecasting sequence. To evaluate the performance of proposed model, three metrics in Eqs. (8)–(8)–(10)(8)–(10) are used, i.e., the mean absolute error (MAE), the mean square error (MSE) and the r-square (R^2).

$$MAE = \frac{1}{n}\sum_{i}^{n}|Y_t - F_t| \tag{8}$$

$$MSE = \frac{1}{n}\sum_{i}^{n}(Y_t - F_t)^2 \tag{9}$$

$$R^2 = 1 - \frac{\sum_{i}^{n}(Y_t - F_t)^2}{\sum_{i}^{n}(\overline{F}_t - F_t)^2} \tag{10}$$

where Y_t, F_t and $\overline{F}_t$ represent the forecast value, the actual value, and the mean of actual values, respectively.

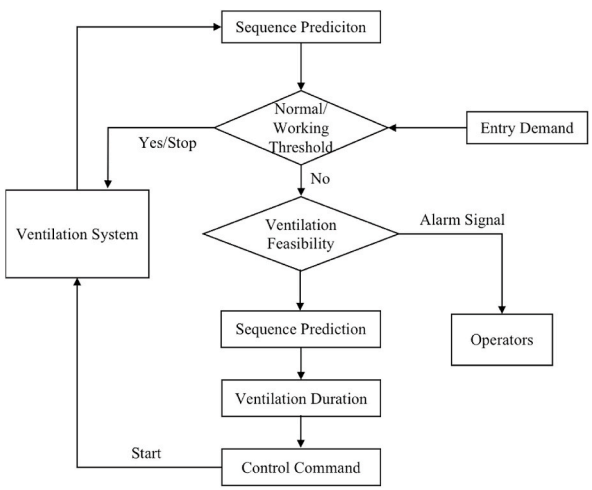

Fig. 6. Intelligent control process of temperature and humidity environment.

3.3. Intelligent ventilation control approach

The intelligent ventilation control approach shown in Fig. 6 for temperature and humidity environment inside utility tunnels is built based on the prediction sequence and the early warning thresholds. The control approach compares the values of the real-time prediction sequence with the early warning thresholds set for the temperature and humidity environment inside utility tunnels. If the forecast value is higher than the upper bound of the threshold or is lower than the lower bound, the approach will judge whether ventilation can address the temperature and humidity abnormities, and sends the early warning information to operators. The feasibility judgment of ventilation is made based on the assumption that the ventilation fans are turned on at the current time, and a simulation prediction sequence of temperature and relative humidity in the future can be obtained. If the predicted sequence shows an effective result, the ventilation duration can then be calculated and the fans control command will be generated and sent to the ventilation system. When the fans are operating, the cooling and de-humidification effects are predicted in real-time until it reaches the accepted range.

4. Experimental case study

4.1. Brief introduction to the utility tunnel project

The experimental case study was conducted in a fire compartment section of a utility tunnel project located in Guizhou Province, China (see Fig. 7). The compartment section is 200 m in length, contains 10 kV power cables, water supply pipelines, communication cable, etc., and has an exhaust fan at the air outlet. A monitoring sensor was installed inside the compartment to collect the temperature and relative humidity data continuously (see Fig. 2). As the fire doors at the two ends normally keep closed, the influence from adjacent compartment sections on the air temperature and relative humidity of the experimental compartment section can be ignored.

4.2. Data preparation

4.2.1. Raw data

Raw data included 11,520 samples that were collected from April 1, 2019 at 0:00 to May 10, 2019 at 24:00 with a collecting frequency of 5 min. In the experiment, 8640 samples collected in April were used for model training, and 2880 samples in May were used for model testing, prediction and performance evaluation. Features in each raw data sample are listed in Table 3. The temperature and relative humidity data collected inside the utility tunnel in April (30 days) for model training are shown in Figs. 8 and 9, respectively.

4.2.2. Data preprocessing

Since this case study only involves one fire compartment without air inlet fans, the fields of Section, Compartment and In_Fan were removed from the raw data in the data preprocessing, and the collection time was used as the sequence index.

4.2.3. Feature engineering

In this experiment, the prediction process used the data sequence of the first 12 time steps (i.e. 1 h) to forecast the temperature and relative humidity values inside the utility tunnel for the next time step. The data input method is called sliding window method. As shown in Fig. 10, the feature engineering process includes the following steps.

① Combine the samples of the first 12 time steps into an input sample. Since each time step contains five features, an input sample contains 60 features.
② The corresponding label vector (expected output value) is the temperature and relative humidity at the 13th time step.
③ Get a Key/Value pair, e.g., (input_sample, label_vector).

Fig. 7. Interior environment of the utility tunnel used for experimental case study.

Table 3
Feature details of raw data.

Feature annotation (data field)	Description	Unit or value
Time	Collecting time of samples	/
Section	Section number in a utility tunnel	/
Compartment	Fire compartment number in a tunnel section	/
Out_Temp	Daily average temperature of external environment	[°C]
Out_Hum	Daily average relative humidity of external environment	[%]
In_Temp	Monitored temperature inside the utility tunnel	[°C]
In_Hum	Monitored relative humidity inside the utility tunnel	[%]
Ex_Fan	Statuses of fans at air outlet	0,1 and - 1 representing stop, start and not installed, respectively
In_Fan	Statuses of fans at air inlet	0,1 and - 1 representing stop, start and not installed, respectively

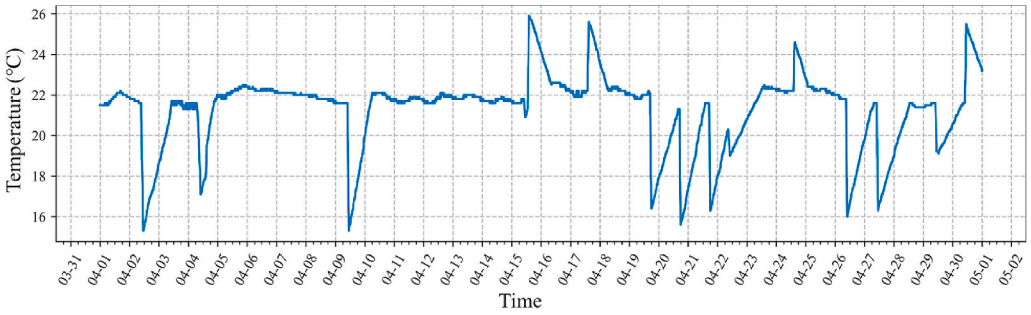

Fig. 8. Temperature data inside the utility tunnel for model training (30 days).

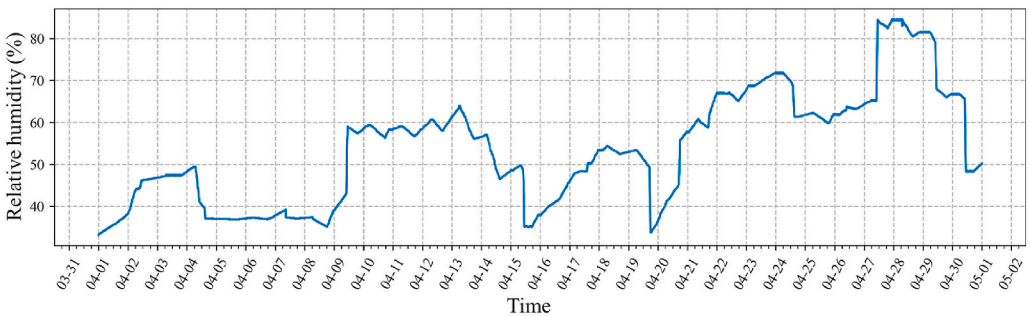

Fig. 9. Relative humidity data inside the utility tunnel for model training (30 days).

④ Then, the input window slides down one item along the time sequence to get the next input sample, that is, taking the value of the second to the 13th time steps as an input sample and the 14th time step value as the label vector.
⑤ In this manner, all datasets are traversed to get the final training dataset and testing dataset.

4.3. Model tuning

In this case study, the proposed LSTM-RNN forecasting architecture was operated on Keras, which is a popular deep learning framework. The activation function adopted the ReLU function (i.e., $f(x) = \max(0, x)$), which is used to add nonlinear factors to the neural network [28].

The model tuning process determines the number of LSTM hidden layers n and the number of hidden variable units based on comparative analysis. The metric of MAE was used during this process. A smaller the value of MAE indicates a better forecasting performance. Model performances under different hidden layers n are listed in Table 4. It is evident that MAE decreased to a low level when n is three and four, but increased sharply when n exceeds four. In order to reduce the number of model parameters and improve forecasting efficiency, the number of hidden layers n was adopted to be three.

In a similar fashion, the number of hidden variable units was adopted as 40 based on the comparison results listed in Table 5. As such, the number of total model parameters in the forecasting architecture reached 33,362.

	var1(t-12)	var2(t-12)	var3(t-12)	var4(t-12)	var5(t-12)	···	var1(t-1)	var2(t-1)	var3(t-1)	var4(t-1)	var5(t-1)
12	0.119084	0.210145	0.0	0.572581	0.441176	···	0.119084	0.210145	0.0	0.580645	0.447059
13	0.119084	0.210145	0.0	0.574597	0.441176	···	0.119084	0.210145	0.0	0.580645	0.447059
14	0.119084	0.210145	0.0	0.576613	0.441176	···	0.119084	0.210145	0.0	0.582661	0.447059
15	0.119084	0.210145	0.0	0.576613	0.441176	···	0.119084	0.210145	0.0	0.582661	0.447059
16	0.119084	0.210145	0.0	0.576613	0.441176	···	0.119084	0.210145	0.0	0.582661	0.447059
...	...	...	...	...	...	...	...	...	...	...	...
8635	0.458015	0.782609	0.0	0.780242	0.576470	···	0.458015	0.782609	0.0	0.782258	0.582353
8636	0.458015	0.782609	0.0	0.780242	0.576470	···	0.458015	0.782609	0.0	0.782258	0.582353
8637	0.458015	0.782609	0.0	0.780242	0.576470	···	0.458015	0.782609	0.0	0.782258	0.582353
8638	0.458015	0.782609	0.0	0.780242	0.576470	···	0.458015	0.782609	0.0	0.782258	0.582353
8639	0.458015	0.782609	0.0	0.780242	0.582353	···	0.458015	0.782609	0.0	0.782258	0.582353

(a) Input sample sequences

	var4(t)	var5(t)
12	0.580645	0.447059
13	0.582661	0.447059
14	0.582661	0.447059
15	0.582661	0.447059
16	0.582661	0.447059
...	...	...
8635	0.782258	0.582353
8636	0.782258	0.582353
8637	0.782258	0.582353
8638	0.782258	0.582353
8639	0.782258	0.582353

(b) Label sequence

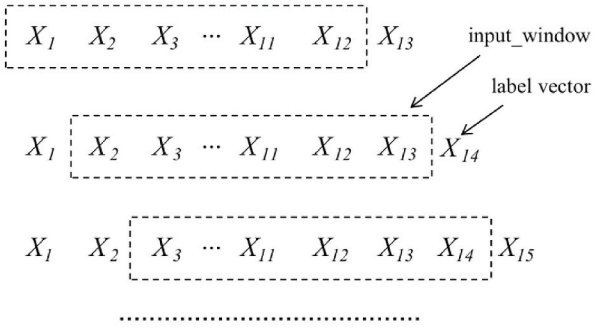

(c) Window sliding method

Fig. 10. Feature engineering process.

Table 4
Model performances under different hidden layers.

Hidden layers (n)	MAE
1	0.218307
2	0.192067
3	0.178054
4	0.177195
5	0.321515

Table 5
Model performances of relative humidity under different units.

Units	Number of model parameters	MAE
10	2342	0.822191
20	8682	0.481932
30	19,022	0.363288
40	33,362	0.313005
50	51,702	0.312945
60	74,042	0.311764

4.4. Results

4.4.1. Model training results

The loss function during the training process used the metric of MSE. One iteration represents a back-propagation process and a model update. Fig. 11 shows that the MSE value of the training model gradually converged as the number of iterations increased, indicating that the trained model fit well on the training dataset.

To verify the forecasting performance of trained model on new data, testing dataset samples were input to calculate the prediction results. Figs. 12 and 13 show that the prediction curves fit well on testing dataset samples. The values of MSE, MAE, R^2 Score were calculated and listed in Table 6. MAE and MSE on the testing dataset were close to zero and R^2 score was close to 1.0, which all met the

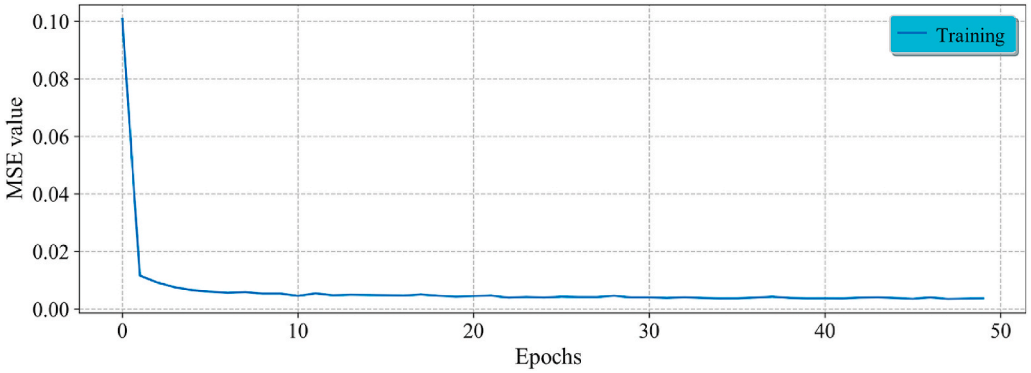

Fig. 11. Loss function curve.

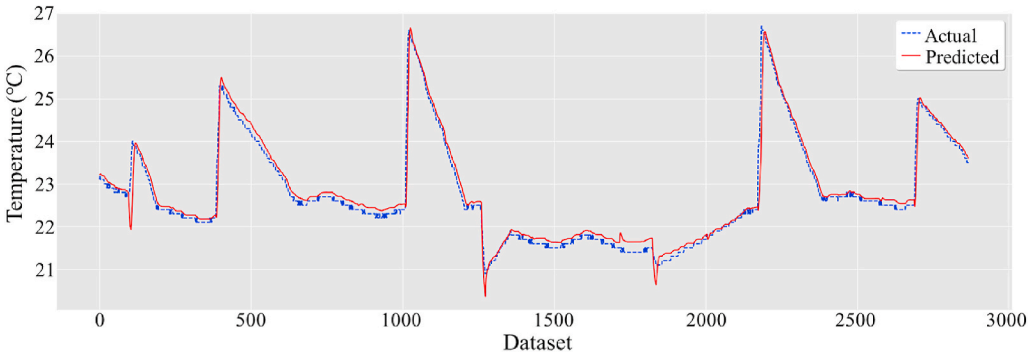

Fig. 12. Comparison between temperature prediction results and actual values.

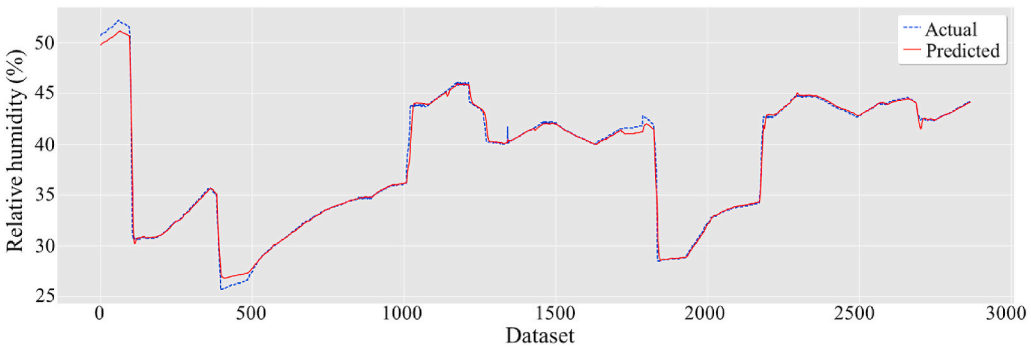

Fig. 13. Comparison between relative humidity prediction results and actual values.

Table 6
Evaluation of the prediction results of test dataset.

Indicator	Temperature (°C)	Relative Humidity (%)
MAE	0.003413	0.006644
MSE	0.024410	0.221719
R^2 Score	0.983622	0.994324

required prediction accuracies.

4.4.2. Intelligent ventilation control

4.4.2.1. Early warning. Fig. 14 shows a prediction sequence of the relative humidity for the experimental section in the next 2 h at the time of 18:45, May 21, 2019 without turning on the fans. According to the prediction sequence, the relative humidity would exceed the warning limit, i.e., the comfort threshold of 70% at the warning level II, at around 20:10, thus the intelligent ventilation control system should send an early warning signal to operators at least 5 min in advance. After receiving the warning signal, utility tunnel operators should pay more attention to the monitoring data of relative humility, while getting prepared to start the ventilation fans. When the relative humidity value reached the prediction point, a high risk warning would be sent accordingly. Subsequently, de-humidification measures must be taken immediately, and patrol personnel should be sent to the corresponding section to find out the causes and check the potential safety hazards such as short circuit and corrosion.

4.4.2.2. Ventilation feasibility assessment. Before the ventilation fans start, the effect on cooling or de-humidification should be assessed by the trained LSTM-RNN model. The first step is to assume the fans to be turned on, then integrate the fans status with the monitoring value of temperature and relative humidity as a new input sample sequence. Similar to the prediction sequence, a simulation curve of temperature or relative humidity can be obtained under the scenario of ventilation. Fig. 15 shows a simulation case of turning on the fans, the forecasted changing curve of temperature revealed that turning on the fans at the time of 8:45 could reduce the temperature inside the experimental utility tunnel from 31.5 °C to 23.6 °C, which achieved the temperature control objective. Thus, it was recommended that the operators turn on the fans as soon as possible since it had been proved a good time for ventilation and cooling. In addition, it can be seen from the figure that the time required for the temperature to reach the control target was about 45 min, which allowed operators to obtain an estimate of the ventilation duration so as to turn off the fans timely to save energy.

4.5. Discussions

Despite the good computational performances in temperature and relative humidity forecasting for utility tunnel indoor atmosphere, it should also be noted that there are some limitations to be addressed in future research. For instance, as the training data obtained in this experimental case study was mainly collected in April, deep features might have not been learnt from it. Therefore, it is necessary to expand the collection time range of the training data (such as one year). Yet for a long prediction sequence, the window sliding method could be called into question in that the prediction errors at each time step can accumulate to a large error. In this sense, further research on new methods for the feature engineering process of long-step forecasting is expected. As regards the ventilation control approach for urban utility tunnels, other indoor atmosphere indicators, such as methane, hydrogen sulfide and other harmful gases, should also be considered, which implies that an integrated control approach is required. In addition, the proposed LSTM-RNN based forecasting architecture is only suited for utility tunnel operational indicators with time-series structures, such as temperature and relative humidity selected in this study. In general terms, however, the risk warning model needs to incorporate a variety of operational indicators into a comprehensive risk index, which means that the risk assessment method and the warning mechanism incorporating other data types should be further studied.

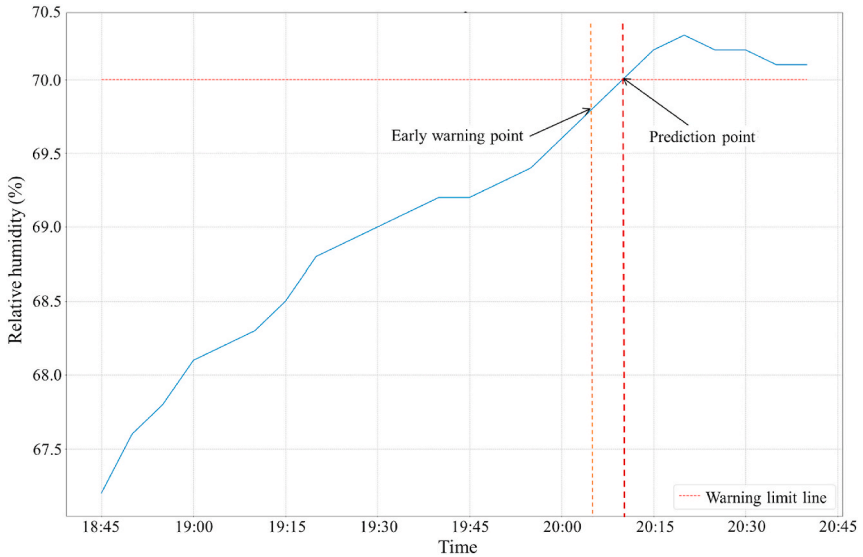

Fig. 14. Early warning of relative humidity inside experimental utility tunnel.

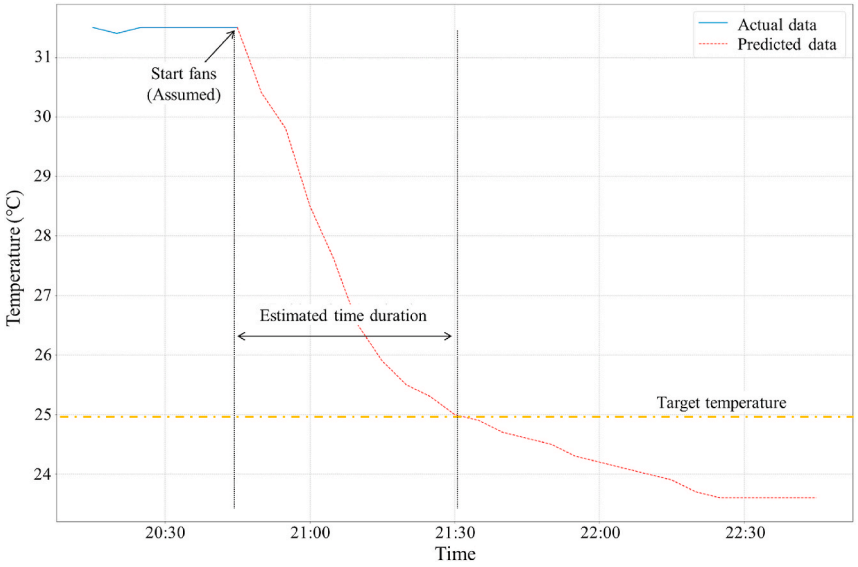

Fig. 15. Ventilation feasibility assessment and control strategy.

5. Conclusion

In order to achieve the safe, efficient and energy-saving control of temperature and humidity environment inside urban utility tunnels, this paper proposed an LSTM-RNN based intelligent forecasting and ventilation control approach. With the aid of an experimental case study, the following conclusions can be drawn :

(1) The proposed LSTM-RNN based architecture can be used to forecast the time series of temperature and humidity in real-time. The prediction sequence reflects the changing trend of temperature and humidity, based on which early warning can be achieved.
(2) After model tuning, when the number of hidden layers was three and the number of LSTM hidden variable units was 40, the overall efficiency of the LSTM RNN model's complexity and computational performance reached the highest in the experimental case study. The prediction accuracy on testing datasets of temperature and relative humidity exceeded 98% and 99%, respectively.
(3) The trained LSTM-RNN model can also be used to simulate the ventilation effect under different conditions. When the ventilation target cannot be achieved, operators should be reminded to use the fans carefully. When it can be satisfied, the required ventilation duration can be estimated and provide instructions to the control system to achieve efficient and energy-saving ventilation control.

Notwithstanding the limitations in training data and indicator selection, the proposed forecasting and ventilation control architecture sets up a solid methodological foundation for future research to address some of the existing limitations and other issues regarding utility tunnel indoor atmosphere hazards and operational risks.

Author contribution statement

Fang-Le Peng: Conceived and designed the experiments; Performed the experiments; Contributed reagents, materials, analysis tools or data.

Yong-Kang Qiao: Conceived and designed the experiments; Analyzed and interpreted the data; Contributed reagents, materials, analysis tools or data; Wrote the paper.

Chao Yang: Conceived and designed the experiments; Performed the experiments; Analyzed and interpreted the data; Contributed reagents, materials, analysis tools or data.

Funding statement

Dr. Yong-Kang Qiao was supported by National Natural Science Foundation of China [42201284], National Postdoctoral Program for Innovative Talents [BX2021220].

Fang-Le Peng was supported by National Natural Science Foundation of China [52090083].

Data availability statement

Data will be made available on request.

Declaration of interest's statement

The authors declare no competing interests.

References

[1] J.J. Cano-Hurtado, J. Canto-Perello, Sustainable development of urban underground space for utilities, Tunn. Undergr. Space Technol. 14 (1999) 335–340.
[2] D.V.L. Hunt, D. Nash, C.D.F. Rogers, Sustainable utility placement via multi-utility tunnels, Tunn. Undergr. Space Technol. 39 (2014) 15–26.
[3] Z.Y. Zhang, F.L. Peng, C.X. Ma, H. Zhang, S.J. Fu, External benefit assessment of urban utility tunnels based on sustainable development, Sustainability 13 (2021) 900.
[4] F.L. Peng, Y.K. Qiao, S. Sabri, B. Atazadeh, A. Rajabifard, A collaborative approach for urban underground space development toward sustainable development goals: critical dimensions and future directions, Front. Struct. Civ. Eng. 15 (1) (2021) 20–45.
[5] Y.K. Qiao, F.L. Peng, X.L. Wu, Y.P. Luan, Visualization and spatial analysis of socio-environmental externalities of urban underground space use: Part 1 positive externalities, Tunn. Undergr. Space Technol. 121 (2022), 104325.
[6] J. Curiel-Esparza, J. Canto-Perello, Indoor atmosphere hazard identification in person entry urban utility tunnels, Tunn. Undergr. Space Technol. 20 (5) (2005) 426–434.
[7] C. Tai, G. Tian, W. Lei, J. Wang, A field measurement of temperature and humidity in a utility tunnel and a brief analysis of the exhaust heat recovery system, Indoor Built Environ. 30 (4) (2021) 487–501.
[8] D. Wu, Y. Zhang, A. Li, et al., Indoor airborne fungal levels in selected comprehensive compartments of the urban utility tunnel in Nanjing, Southeast China, Sustain. Cities Soc. 51 (2019), 101723.
[9] Y. Zhang, D. Wu, Q. Kong, et al., Exposure level and distribution of airborne bacteria and fungi in an urban utility tunnel: a case study, Tunn. Undergr. Space Technol. 96 (2020), 103215.
[10] Y.P. Bai, R. Zhou, J. Wu, Hazard identification and analysis of urban utility tunnels in China, Tunn. Undergr. Space Technol. 106 (2020), 103584.
[11] L. He, G. Ma, Q. Hu, et al., A novel method for risk assessment of cable fires in utility tunnel, Math. Probl Eng. 2019 (2019), 2563012.
[12] K. Ye, X. Tang, Y. Zheng, et al., Estimating the two-dimensional thermal environment generated by strong fire plumes in an urban utility tunnel, Process Saf. Environ. Protect. 148 (2021) 737–750.
[13] Q. Qi, S.M. Deng, Multivariable control of indoor air temperature and humidity in a direct expansion (DX) air conditioning (A/C) system, Build. Environ. 44 (8) (2009) 1659–1667.
[14] P. Zhang, H.Q. Lan, Effects of ventilation on leakage and diffusion law of gas pipeline in utility tunnel, Tunn. Undergr. Space Technol. 105 (2020), 103557.
[15] C.D. Liu, S. Li, H.H. Tang, Y.Q. Xie, C. Xiang, Similarity analysis on the ventilating reduced-scale model of urban underground utility tunnel, Chin. J. Undergr. Space Eng. 15 (6) (2019) 1609–1619 (in Chinese).
[16] L. Shu, X. Liu, J. Wang, et al., Reduced scale experimental study and CFD analysis on the resistance characteristic of utility tunnel's ventilation system, Energy Proc. 158 (2019) 2756–2761.
[17] I. Shahrour, H. Bian, X. Xie, et al., Use of smart technology to improve management of utility tunnels, Appl. Sci. 10 (2) (2020) 711.
[18] H. Yang, Y.F. Yan, X.R. Lu, Ventilation system design of urban utility tunnel based on fuzzy PID control algorithm, Control Eng. China 26 (12) (2019) 2181–2187 (in Chinese).
[19] J.J. Hopfield, Neural networks and physical systems with emergent collective computational abilities, Proc. Natl. Acad. Sci. USA 79 (8) (1982) 2554–2558.
[20] S. Hochreiter, J. Schmidhuber, Long short-term memory, Neural Comput. 9 (8) (1997) 1735–1780.
[21] S.S. Lin, S.L. Shen, A.N. Zhou, Real-time analysis and prediction of shield cutterhead torque using optimized gated recurrent unit neural network, J. Rock Mech. Geotech. Eng. 14 (4) (2022) 1232–1240.
[22] S.V. Belavadi, S. Rajagopal, R. Ranjani, et al., Air quality forecasting using LSTM RNN and wireless sensor networks, Procedia Comput. Sci. 170 (2020) 241–248.
[23] S. Zhang, H. Ma, X. Huang, S. Peng, Numerical simulation on methane-hydrogen explosion in gas compartment in utility tunnel, Process Saf. Environ. Protect. 140 (2020) 100–110.
[24] MoHURD (Ministry of Housing and Urban-Rural Development of P.R.China, Technical Standard for Operation, Maintenance and Safety Management of Urban Utility Tunnel, GB, 2019, pp. 51354–52019 (in Chinese).
[25] MoH (Ministry of Health of P.R.China, Specification of Prevention and Control on Occupational Hazards in Confined Space, 2007. GBZ T205-2007. (in Chinese).
[26] F. Mtibaa, K.K. Nguyen, M. Azam, et al., LSTM-based indoor air temperature prediction framework for HVAC systems in smart buildings, Neural Comput. Appl. 32 (2020) 17569–17585.
[27] D. Kingma, J. Ba, Adam, a method for stochastic optimization. http://arxiv.org/abs/1412.6980.
[28] S.L. Shen, N. Zhang, A. Zhou, Z.Y. Yin, Enhancement of neural networks with an alternative activation function tanhLU, Expert Syst. Appl. 199 (2022), 117181.